

## Supporting Information

### Formation of a Meltable Purinate Metal—Organic Framework and its Glass Analogue

Alice M. Bumstead,<sup>a</sup> Celia Castillo-Blas,<sup>a</sup> Ignas Pakamorè,<sup>b</sup> Michael F. Thorne,<sup>a</sup> Adam F. Sapnik,<sup>a</sup> Ashleigh M. Chester,<sup>a</sup> Georgina Robertson,<sup>a</sup> Daniel J. M. Irving,<sup>c</sup> Philip A. Chater,<sup>c</sup> David A. Keen,<sup>d</sup> Ross S. Forgan,<sup>b</sup> and Thomas D. Bennett<sup>a\*</sup>

Contact email: [tdb35@cam.ac.uk](mailto:tdb35@cam.ac.uk)

- a. Department of Materials Science and Metallurgy, University of Cambridge, Cambridge, CB3 0FS, UK.
- b. WestCHEM, School of Chemistry, University of Glasgow, University Avenue, Glasgow, G12 8QQ, UK.
- c. Diamond Light Source Ltd, Diamond House, Harwell Campus, Didcot, Oxfordshire, OX11 0DE, UK.
- d. ISIS Facility, Rutherford Appleton Laboratory, Harwell Campus, Didcot, Oxfordshire, OX11 0QX, UK.

# Contents List

## Methods

### Figures

<b>Fig. S1</b>	Reaction scheme for the formation of ZIF-UC-7.	5
<b>Fig. S2</b>	Single crystals of ZIF-UC-7.	5
<b>Fig. S3</b>	Powder X-ray diffraction patterns of ZIF-UC-7 and $a_g$ ZIF-UC-7.	6
<b>Fig. S4</b>	Scanning electron microscope images of crystalline ZIF-UC-7 powder.	6
<b>Fig. S5</b>	Pawley refinement of powder X-ray diffraction data of ZIF-UC-7.	7
<b>Fig. S6</b>	$^1\text{H}$ nuclear magnetic resonance spectrum of ZIF-UC-7.	7
<b>Fig. S7</b>	Thermogravimetric analysis of crystalline ZIF-UC-7 to 1000 °C.	8
<b>Fig. S8</b>	Differential scanning calorimetry of crystalline ZIF-UC-7.	8
<b>Fig. S9</b>	$^1\text{H}$ nuclear magnetic resonance spectrum of ZIF-UC-7 post 400 °C.	9
<b>Fig. S10</b>	DSC of crystalline ZIF-UC-7 with in-situ activation step.	10
<b>Fig. S11</b>	Analysis of DSC of crystalline ZIF-UC-7 with in-situ activation step.	10
<b>Fig. S12</b>	$^1\text{H}$ nuclear magnetic resonance spectrum of ZIF-UC-7 post 350 °C.	11
<b>Fig. S13</b>	Powder X-ray diffraction patterns of ZIF-UC-7 heated to 250-450 °C.	11
<b>Fig. S14</b>	X-ray total scattering data for ZIF-UC-7 and $a_g$ ZIF-UC-7.	12
<b>Fig. S15</b>	$\text{CO}_2$ adsorption and desorption isotherms collected on crystalline ZIF-UC-7.	12
<b>Fig. S16</b>	$\text{CO}_2$ adsorption and desorption isotherms collected on $a_g$ ZIF-UC-7.	13
<b>Fig. S17</b>	Enthalpy and entropy of fusion of ZIF-UC-7 compared to other ZIFs.	13

### Tables

<b>Table S1</b>	Crystal data and structure refinement for ZIF-UC-7.	5
<b>Table S2</b>	Data from Pawley refinement of ZIF-UC-7.	7
<b>Table S3</b>	CHN Microanalysis of crystalline ZIF-UC-7.	9
<b>Table S4</b>	CHN Microanalysis of $a_g$ ZIF-UC-7.	9
<b>Table S5</b>	$\text{CO}_2$ gas sorption results for crystalline ZIF-UC-7.	12
<b>Table S6</b>	$\text{CO}_2$ gas sorption results for $a_g$ ZIF-UC-7.	13
<b>Table S7</b>	Melting thermodynamics of ZIF-UC-7 vs. reported values for other ZIFs.	14

## References

## Methods

**Materials:** Imidazole ( $\geq 99.5\%$ ), D<sub>2</sub>O (35 wt.% DCl) and purine (98%) were purchased from Sigma Aldrich. Dimethyl sulfoxide (DMSO)-*d*<sub>6</sub> (99.8 atom% D, contains 0.03% (v/v) tetramethylsilane (TMS)) was purchased from VWR. Zinc nitrate hexahydrate (98%) was purchased from Alfa Aesar. N,N-Dimethylformamide (DMF) (99.5%), and dichloromethane stabilised with amylene (DCM) (99.8%) were purchased from Fischer Scientific. All materials were used without further purification.

**Synthesis of ZIF-UC-7:** Zinc nitrate hexahydrate (1.515 g, 5.09 mmol), imidazole (7.350 g, 108 mmol) and purine (1.441 g, 12.0 mmol) were dissolved in DMF (75 mL) to give an orange/brown colored solution. This solution was heated to 130 °C and held there for 48 hr in an oven before being removed and left to cool to room temperature naturally. The resulting, orange-coloured crystals were isolated by vacuum filtration and washed with fresh DMF. The crystals were then soaked in DCM (5 mL) for 24 hr to allow solvent exchange to take place. The crystals were again isolated by vacuum filtration before being activated under vacuum at 170 °C for 3 hr. This synthetic method was designed based on the reported synthesis of ZIF-UC-6.<sup>1</sup>

**Preparation of ZIF-UC-7 powder.** ZIF-UC-7 (*ca.* 100 mg) was placed inside a stainless-steel ball mill jar along with two 5 mm stainless-steel balls. The jar was sealed and milled at 20 Hz for 5 mins. The resulting cream coloured powder was then soaked in DCM (5 mL) for 24 hr to allow solvent exchange to take place. The crystals were again isolated by vacuum filtration before being activated under vacuum at 170 °C for 3 hr.

**Single Crystal X-ray Diffraction (SCXRD).** Single crystal diffraction data were collected using a Bruker D8 VENTURE diffractometer equipped with a Bruker PHOTON II detector at 150 K using graphite monochromated Mo K $\alpha$  radiation ( $\lambda = 0.71073$ ). Data reduction was done using the APEX3 program. Absorption correction based on multi-scan was obtained by SADABS. The structure was solved and refined using SHELXT and SHELXL packages correspondingly, using the OLEX2 program.<sup>2-4</sup> The electron density within the voids was accounted for using the SQUEEZE program implemented in PLATON.<sup>5</sup>

Crystal data for ZIF-UC-7: C<sub>13</sub> H<sub>12</sub> N<sub>9</sub> Zn<sub>2</sub>,  $M_r = 425.06$ , crystal dimensions 0.62 x 0.51 x 0.32 mm, Orthorhombic,  $a = 15.1336(5)$  Å,  $b = 15.4532(5)$  Å,  $c = 18.4151(6)$  Å,  $\alpha = \beta = \gamma = 90^\circ$ ,  $V = 4306.6(2)$  Å<sup>3</sup>, space group *Pbca*, (No. 61),  $T = 150$  K,  $Z = 8$ , 36647 measured reflections, 5181 independent reflections ( $R_{\text{int}} = 0.060$ ), which were used in all calculations. The final  $R_1 = 0.037$  for 4155 observed data [ $R[F^2 > 2\sigma(F^2)]$ ] and  $wR(F^2) = 0.099$  (all data). CCDC deposition number: 2209865.

**Powder X-ray Diffraction (PXRD).** Data were collected on a Bruker D8 ADVANCE diffractometer equipped with a position sensitive LynxEye detector with Bragg-Brentano parafocusing geometry. Cu K $\alpha$  ( $\lambda = 1.5418$  Å) radiation was used. The samples were compacted into 5 mm disks on a low background silicon substrate and rotated during data collection in the  $2\theta$  range of 5–40° at ambient temperature. All data conversion from .raw files to .xy files was performed using PowDLL.<sup>6</sup> Pawley refinements were performed using TOPAS-Academic Version 6.<sup>7</sup> Thompson-Cox-Hastings pseudo-Voigt (TCHZ) peaks shapes were used along with a simple axial divergence correction. The lattice parameters were refined in the  $2\theta$  range of 5–40° against the values obtained from the CIF for ZIF-UC-7 reported in this work. The zero-point error was also refined.

**Differential Scanning Calorimetry (DSC).** Data were collected on a Netzsch DSC 214 Polyma Instrument. Heating and cooling rates of 10 °C min<sup>-1</sup> were used along with a flowing argon atmosphere. Sealed aluminium pans (30  $\mu$ L) were used with a hole punctured in the lid to prevent pressure build-up. An empty aluminium pan was used as a reference. Background corrections were performed using the same heating cycle on an empty aluminium crucible. All data analysis was performed using the Netzsch Proteus<sup>®</sup> software package.  $T_m$  was taken as the offset (the end point) of the melting endotherm.  $T_g$  was taken as the mid-point of the change in gradient of the heat flow of the DSC on the 2<sup>nd</sup> upscan. The fusion enthalpy ( $\Delta H_{fus}$ ) was obtained from the calculated area of the  $T_m$  peak in J/g and transformed into KJ/mol, according eq. 1. The fusion entropy ( $\Delta S_{fus}$ ) was calculated from equation 2, being  $T = T_m$ .

$$\Delta H_{fus} = \int_{T_0}^{T_1} C_p dT \quad (\text{equation 1})$$

$$\Delta S_{fus} = \frac{\Delta H_{fus}}{T} \quad (\text{equation 2})$$

**Thermogravimetric Analysis (TGA).** Data were collected on a TA Instruments SDT-Q650 using alumina pans (90  $\mu\text{L}$ ). Heating and cooling rates of  $10\text{ }^\circ\text{C min}^{-1}$  were used, and experiments were conducted under a flowing argon atmosphere. All data analysis was performed using the TA Instruments Universal Analysis software package. The temperature used to define any weight changes was determined using the first derivative of the weight (%) trace as a function of temperature.

**$^1\text{H}$  Nuclear Magnetic Resonance (NMR) Spectroscopy.**  $^1\text{H}$  NMR spectra were recorded at 298 K using a Bruker AVIII 500 MHz Spectrometer with a dual  $^{13}\text{C}/^1\text{H}$  (DCH) cryoprobe at the Department of Chemistry, University of Cambridge. Samples of crystalline ZIF-UC-7 and  $a_g\text{ZIF-UC-7}$  were dissolved in a mixture of  $\text{DCl}$  (35%)/ $\text{D}_2\text{O}$  and  $\text{DMSO-}d_6$  in a 1:5 ratio with tetramethylsilane (TMS) used as a reference. All data processing was performed using the Bruker TopSpin 4.0.7 software package.

**$\text{CO}_2$  Gas Sorption:** Measurements were performed on a Micromeritics ASAP 2020 surface area and porosity analyser. Samples of ZIF-UC-7 (95 mg) and  $a_g\text{ZIF-UC-6}$  (78 mg) were degassed by heating under vacuum at  $100\text{ }^\circ\text{C}$  for 12 hr before analysis using carbon dioxide gas at 273 K. Gas uptake was determined using the Micromeritics MicroActive software package.

**Scanning Electron Microscopy (SEM):** SEM images were collected with a high-resolution scanning electron microscope FEI Nova Nano SEM 450, accelerating voltage 15 kV. Samples were prepared by dispersing the material onto double sided adhesive conductive carbon tape that was attached to a flat aluminium sample holder and coated with a platinum layer of 15 nm.

**CHN Microanalysis:** CHN combustion analysis experiments were performed using a CE440 Elemental Analyser, EAI Exeter Analytical Inc. 1.5-2.8 mg of sample was used for each run and three measurements were collected per sample.

**X-ray Total Scattering – Pair Distribution Function (PDF).** X-ray total scattering data were collected at beamline I15-1, Diamond Light Source, UK (EE20038) on crystalline ZIF-UC-7 and glass  $a_g\text{ZIF-UC-7}$ . Both samples were ground and loaded into borosilicate glass capillaries (0.78 mm inner diameter) to a height of 3.9 cm. The capillaries were then sealed before being mounted onto the beamline. Total scattering data were collected at room temperature for the background (*i.e.*, empty instrument), empty borosilicate capillary and for both samples in a  $Q$  range of  $0.4 - 26.0\text{ \AA}^{-1}$  ( $\lambda = 0.189578\text{ \AA}$ , 65.40 keV). The total scattering data were processed to account for absorption corrections and various scattering corrections – background scattering, multiple scattering, container scattering and Compton scattering – in a  $Q$  range of  $0.6 - 26.0\text{ \AA}^{-1}$ . The crystallographic density of ZIF-UC-7 was taken as the density for both ZIF-UC-7 and  $a_g\text{ZIF-UC-7}$  during the data processing. Subsequent Fourier transformation of the processed total scattering data resulted in a real space pair distribution function  $G(r)$  for each material. In this work, we use the  $D(r)$  form of the pair distribution function to accentuate high  $r$  correlations. All processing of the total scattering data was performed using GudrunX following well documented procedures.<sup>8-10</sup>

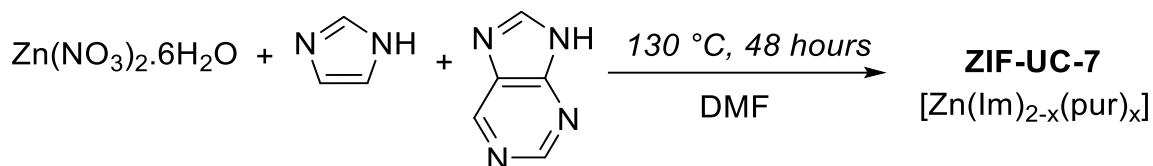


**Figure S1:** Reaction scheme for the formation of ZIF-UC-7 from zinc nitrate hexahydrate, imidazole, and purine under solvothermal conditions.

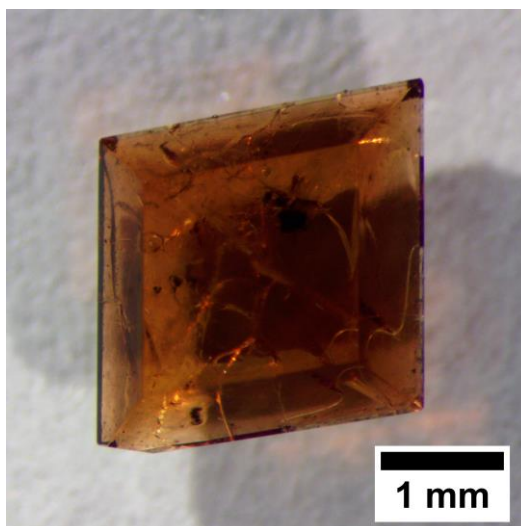


**Figure S2:** Optical microscope image of ZIF-UC-7 single crystal. Scale bar added using ImageJ 1.52.<sup>11</sup>

**Table S1:** Crystal data and structure refinement for ZIF-UC-7.

CCDC number	2209865
Chemical formula	C <sub>13</sub> H <sub>12</sub> N <sub>9</sub> Zn <sub>2</sub>
Formula weight	425.06 g/mol
Temperature	150 K
Wavelength	0.71073 Å
Crystal system	Orthorhombic
Space group	<i>Pbca</i>
Unit cell dimensions	$a = 15.1336(5)$ Å $\alpha = 90^\circ$ $b = 15.4532(5)$ Å $\beta = 90^\circ$ $c = 18.4151(6)$ Å $\gamma = 90^\circ$
Volume	4306.6(2) Å <sup>3</sup>
Density (calculated)	1.311 g/cm <sup>3</sup>
Absorption coefficient	2.24
<i>F</i> (000)	1704
Crystal size	0.62 x 0.51 x 0.32 mm <sup>3</sup>
Theta range for data collection	2.692 – 28.26°
Index ranges	-18 ≤ <i>h</i> ≤ 20, -20 ≤ <i>k</i> ≤ 20, -24 ≤ <i>l</i> ≤ 22
Reflections collected	36647
Independent reflections	5181
Absorption correction	multi-scan
Final <i>R</i> indices [ <i>R</i> [ <i>F</i> <sup>2</sup> > 2σ( <i>F</i> <sup>2</sup> )]	<i>R</i> <sub>1</sub> = 0.037 (4155 observed data)
Final <i>R</i> indices (all data)	<i>wR</i> ( <i>F</i> <sup>2</sup> ) = 0.099

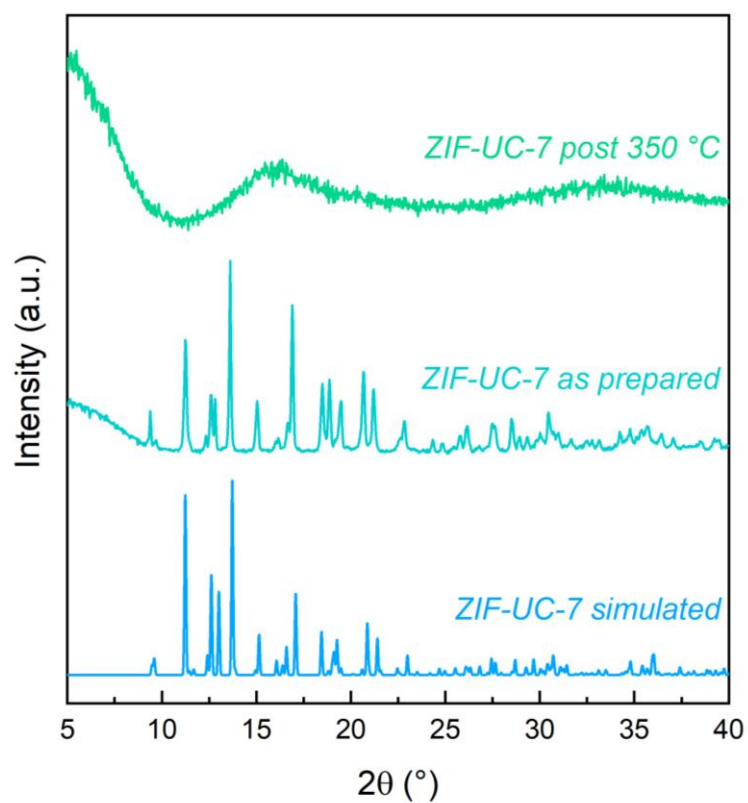


**Figure S3:** Powder X-ray diffraction patterns between 5-40° of as prepared ZIF-UC-7 (cyan) and  $a_g$ ZIF-UC-7 (green) (after heating to 350 °C) compared to the simulated diffraction pattern of ZIF-UC-7 (light blue) obtained from the CIF reported in this work. Conversion of .raw files to .xy files was performed using PowDLL.<sup>6</sup>

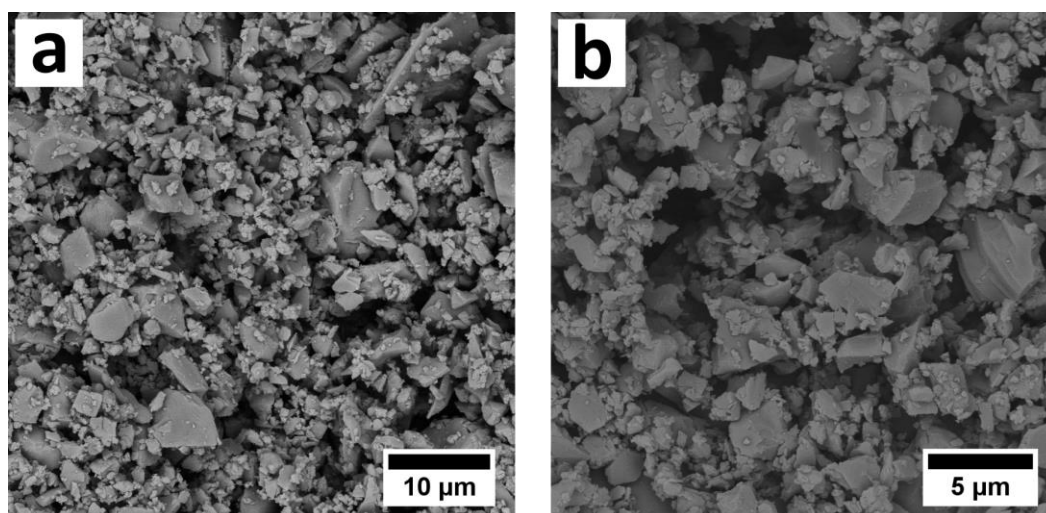


**Figure S4:** Scanning electron microscope images of ZIF-UC-7 powder.

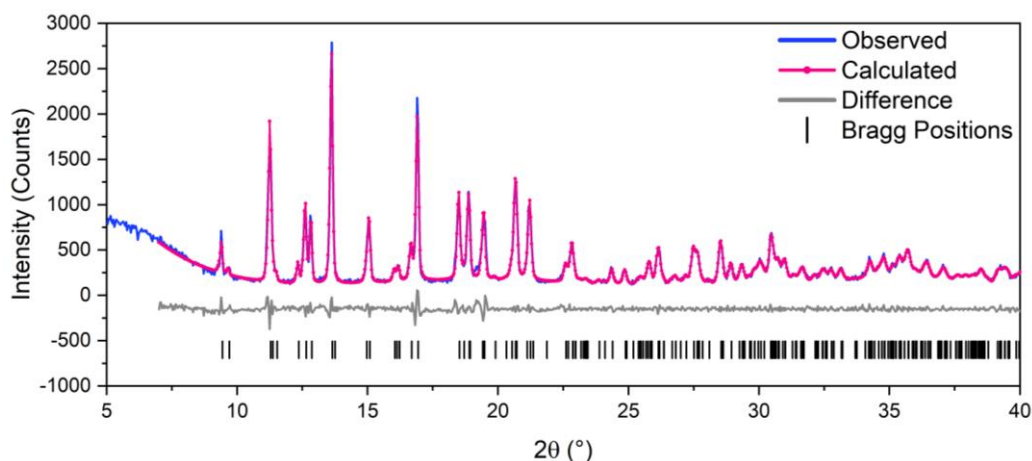


**Figure S5:** Pawley refinement of powder X-ray diffraction data of ZIF-UC-7. Initial parameters were obtained from the CIF for ZIF-UC-7 reported in this work. Conversion of .raw files to .xy files was performed using PowDLL and all powder refinements were performed using TOPAS-Academic Version 6.<sup>6,7</sup> The difference curve and Bragg positions are offset on the y axis for clarity.

**Table S2:** Data from Pawley refinement of ZIF-UC-7

$R_{wp}$	Space Group	Lattice Parameters	Lattice Parameters for ZIF-UC-7
7.799	<i>Pbca</i>	$a = 15.332(3) \text{ \AA}$ $b = 15.545(3) \text{ \AA}$ $c = 18.216(4) \text{ \AA}$ $\alpha = \beta = \gamma = 90^\circ$	$a = 15.1336(5) \text{ \AA}$ $b = 15.4532(5) \text{ \AA}$ $c = 18.4151(6) \text{ \AA}$ $\alpha = \beta = \gamma = 90^\circ$

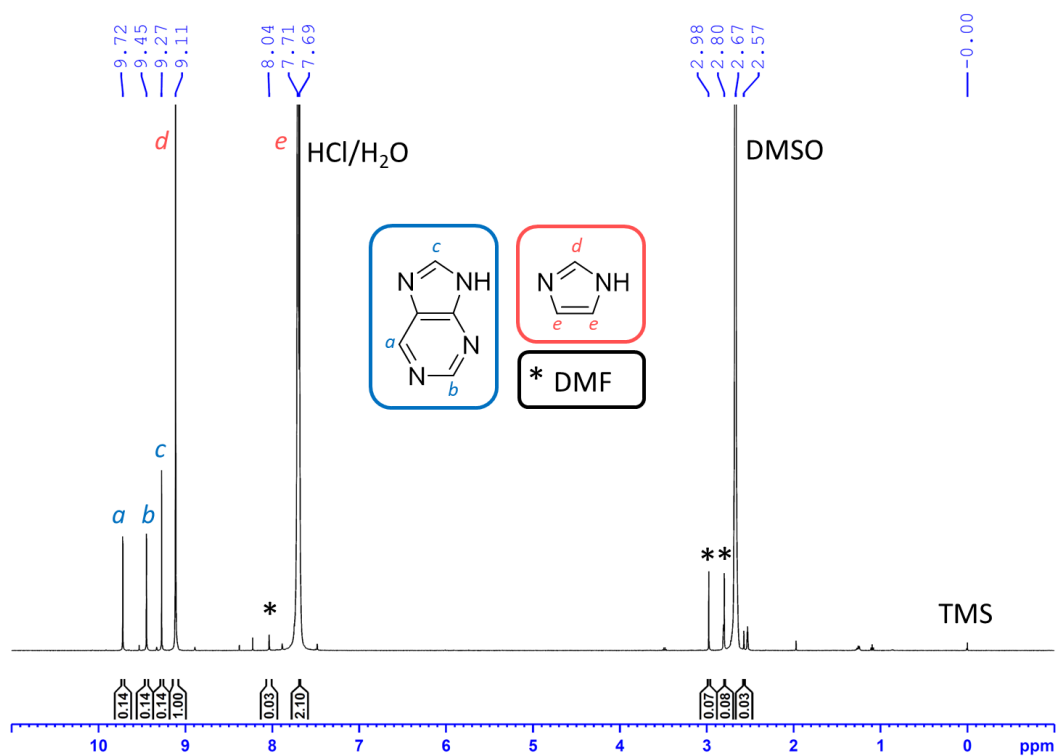


**Figure S6:**  $^1\text{H}$  nuclear magnetic resonance (NMR) spectrum of ZIF-UC-7. All analysis was performed using Topspin Version 4.0.7.  $\delta\text{H}$  (500 MHz;  $\text{DCI}(35\%)/\text{D}_2\text{O}:\text{DMSO}-d_6$  (1:5);  $\text{Me}_4\text{Si}$ ) 9.72 (1H, s,  $\text{H}_a$ ), 9.45 (1H, s,  $\text{H}_b$ ), 9.27 (1H, s,  $\text{H}_c$ ), 9.11 (1H, s,  $\text{H}_d$ ), 8.04 (DMF), 7.71 (2H, s,  $\text{H}_e$ ), 7.69 ( $\text{H}_2\text{O}/\text{HCl}$ ), 2.98, 2.80 (DMF), 2.67 (DMSO), 0.00 (TMS).

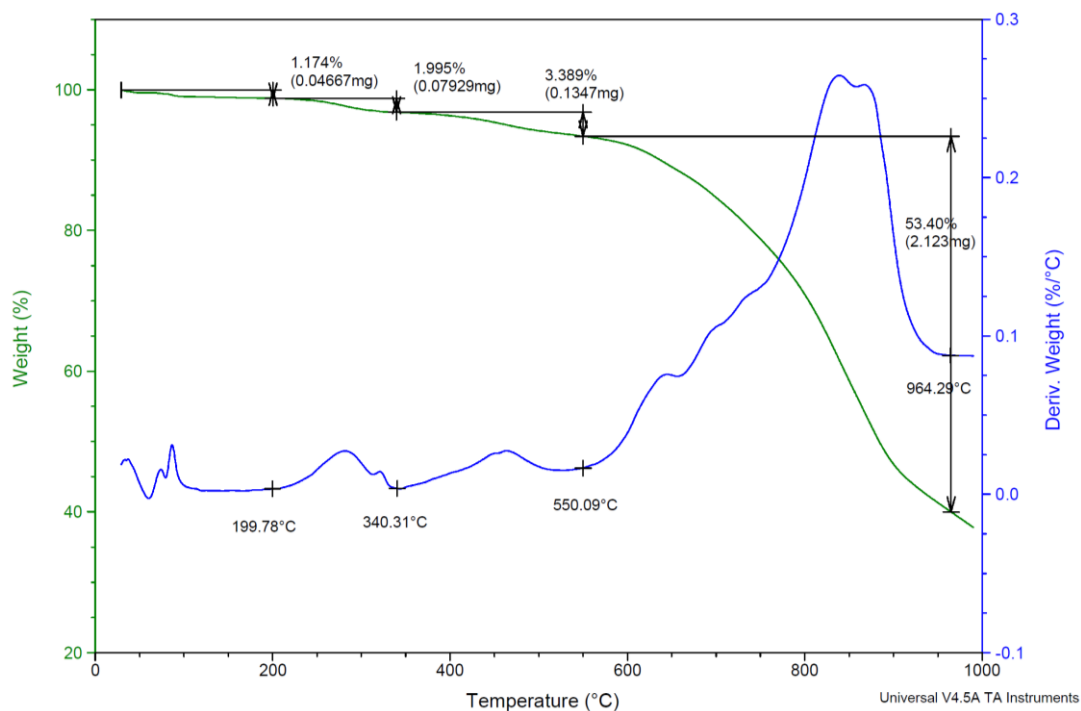


**Figure S7:** Thermogravimetric analysis of crystalline ZIF-UC-7 heated at 10 °C min<sup>-1</sup> up to 1000 °C under argon. Weight (%) curve shown in green and derivative weight (%/°C) shown in blue. Data were collected on a TA Instruments Q650 SDT. All data analysis was performed using the TA Instruments Universal Analysis software package. Weight loss at 340 °C (~2%) and 550 °C correspond to dimethylformamide and partial decomposition of purinate linker, respectively.

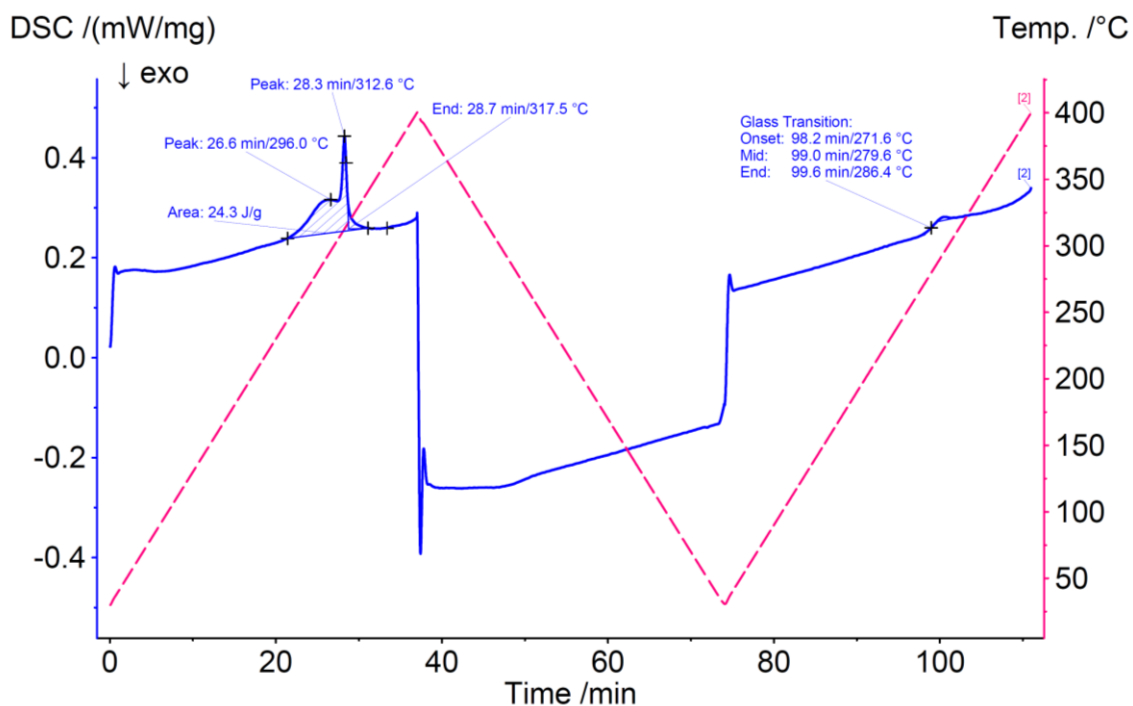


**Figure S8:** Differential scanning calorimetry (DSC) of crystalline ZIF-UC-7 heated to 400 °C, cooled to 30 °C and heated to 400 °C at 10 °C min<sup>-1</sup> under argon. Heat flow curve shown in blue and temperature trace shown in pink. Data were collected on a Netzsch DSC 214 Polyma Instrument. All data analysis was performed using the Netzsch Proteus® software package.

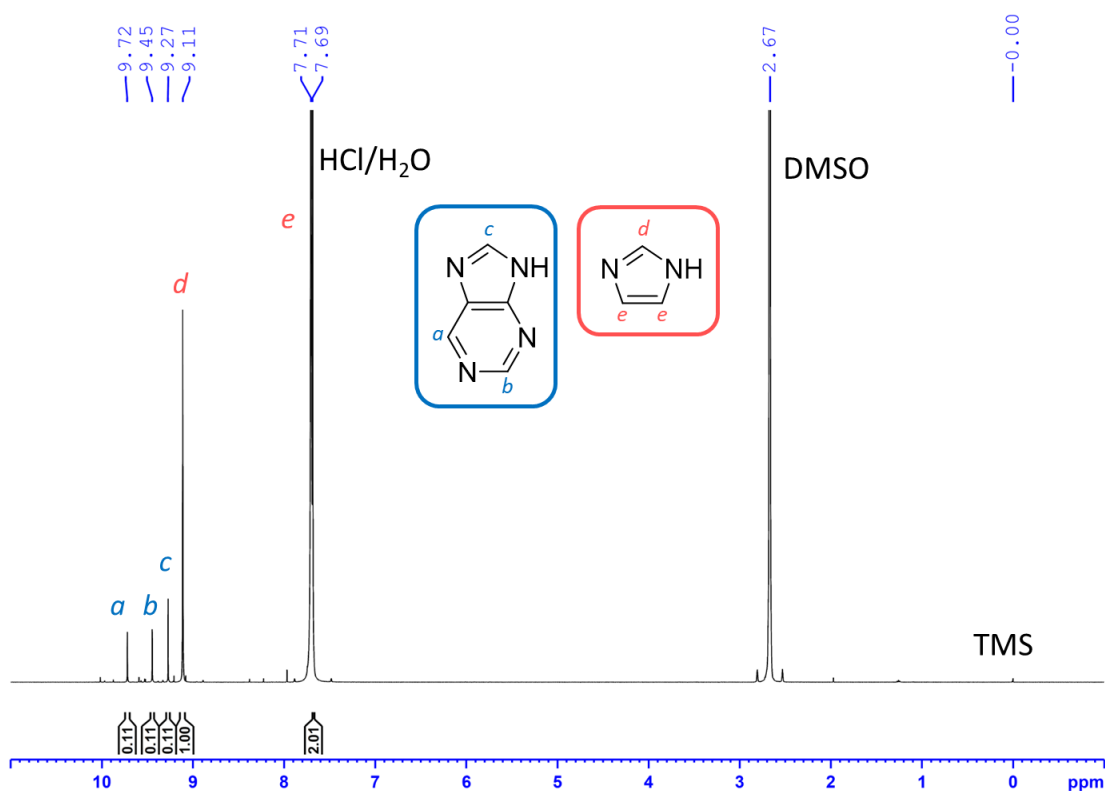


**Figure S9:** <sup>1</sup>H NMR spectrum of ZIF-UC-7 post 400 °C. δH (500 MHz; DCl(35%)/D<sub>2</sub>O:DMSO-d<sub>6</sub> (1:5); Me<sub>4</sub>Si) 9.72 (1H, s, H<sub>a</sub>), 9.45 (1H, s, H<sub>b</sub>), 9.27 (1H, s, H<sub>c</sub>), 9.11 (1H, s, H<sub>d</sub>), 7.71 (2H, s, H<sub>e</sub>), 7.69 (H<sub>2</sub>O/HCl), 2.67 (DMSO), 0.00 (TMS).

**Table S3:** CHN microanalysis of ZIF-UC-7 and comparison with the calculated formula

Sample	Mass (mg)	wt.% C	wt.% H	wt.% N
ZIF-UC-7	1.5296	36.35	2.34	28.16
ZIF-UC-7	1.6124	36.35	2.37	28.17
ZIF-UC-7	2.7858	36.30	2.38	28.19
Mean (ESD)	-	36.33 (0.03)	2.36 (0.02)	28.17 (0.02)
[Zn(pur) <sub>0.25</sub> (Im) <sub>1.75</sub> ]	-	36.43	3.65	29.41

**Table S4:** CHN microanalysis of α<sub>g</sub>ZIF-UC-7 obtained after a thermal heating at 400 °C and comparison with the calculated formula. Discrepancies are due starting of decomposition of the purinate linker over 350 °C.

Sample	Mass (mg)	wt.% C	wt.% H	wt.% N
α <sub>g</sub> ZIF-UC-7	1.8166	35.41	2.69	27.42
α <sub>g</sub> ZIF-UC-7	1.8835	35.42	2.53	27.25
α <sub>g</sub> ZIF-UC-7	2.3379	35.43	2.54	27.34
Mean (ESD)	-	35.42 (0.01)	2.59 (0.08)	27.34 (0.11)
[Zn(pur) <sub>0.25</sub> (Im) <sub>1.75</sub> ]	-	36.43	3.65	29.41

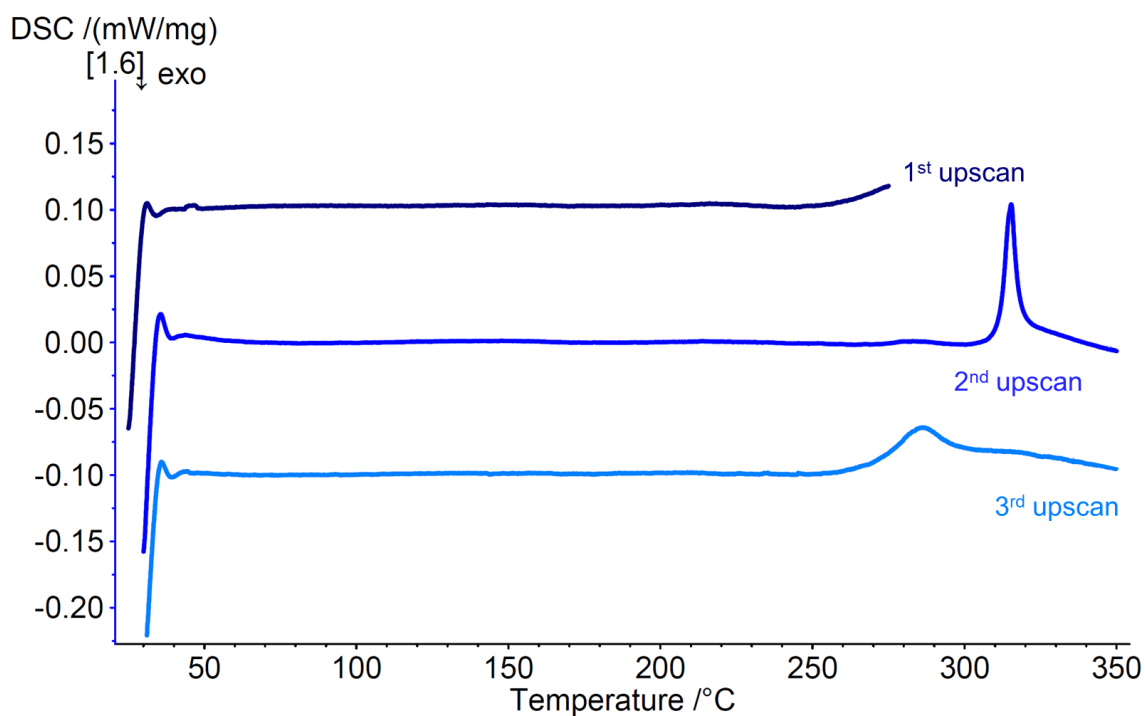


**Figure S10:** DSC of crystalline ZIF-UC-7 with *in-situ* activation step. A sample of ZIF-UC-7 was heated to 275 °C for 5 minutes, cooled to 30 °C, heated to 350 °C, cooled to 30 °C then reheated to 350 °C. All scans were performed at 10 °C min<sup>-1</sup> under argon. Heat flow curves shown are 1<sup>st</sup> upscan to 275 °C (dark blue), 2<sup>nd</sup> upscan to 350 °C (blue) and 3<sup>rd</sup> upscan to 350 °C (light blue). Heat flow curves are offset on the y axis for clarity.

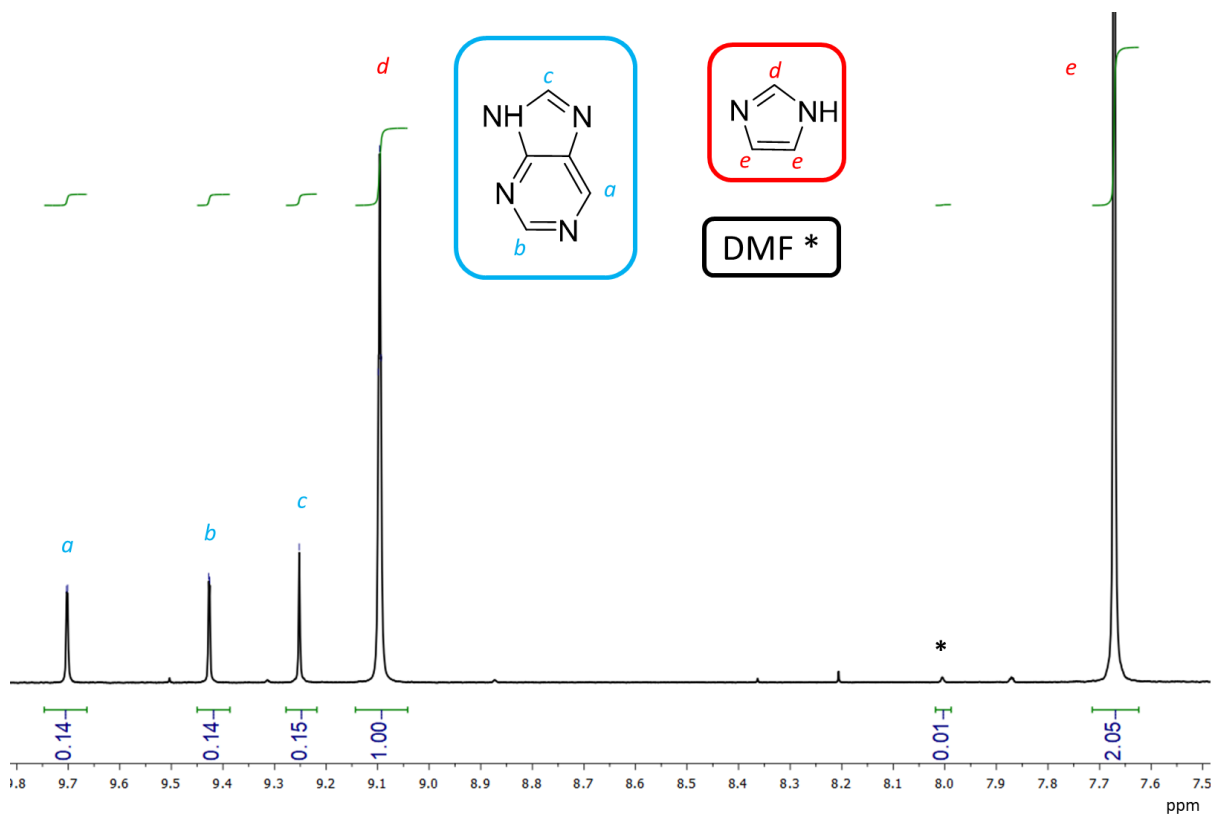


**Figure S11:** <sup>1</sup>H NMR spectrum of ZIF-UC-7 post 275 °C. δH (500 MHz; DCl(35%)/D<sub>2</sub>O:DMSO-d<sub>6</sub> (1:5); Me<sub>4</sub>Si) 9.70 (1H, s, H<sub>a</sub>), 9.43 (1H, s, H<sub>b</sub>), 9.25 (1H, s, H<sub>c</sub>), 9.09 (1H, s, H<sub>d</sub>), 7.67 (2H, s, H<sub>e</sub>), 7.09 (H<sub>2</sub>O/HCl), 2.67 (DMSO), 0.00 (TMS).

**Table S5:** CHN microanalysis of ZIF-UC-7 heated at 275 °C and comparison with the calculated formula

Sample	Mass (mg)	wt.% C	wt.% H	wt.% N
ZIF-UC-7	1.5296	36.35	2.34	28.16
ZIF-UC-7	1.6124	36.35	2.37	28.17
ZIF-UC-7	2.7858	36.30	2.38	28.19
Mean (ESD)	-	36.15 (0.02)	2.36 (0.02)	28.17 (0.02)
[Zn(pur) <sub>0.25</sub> (Im) <sub>1.75</sub> ]	-	36.43	3.65	29.41

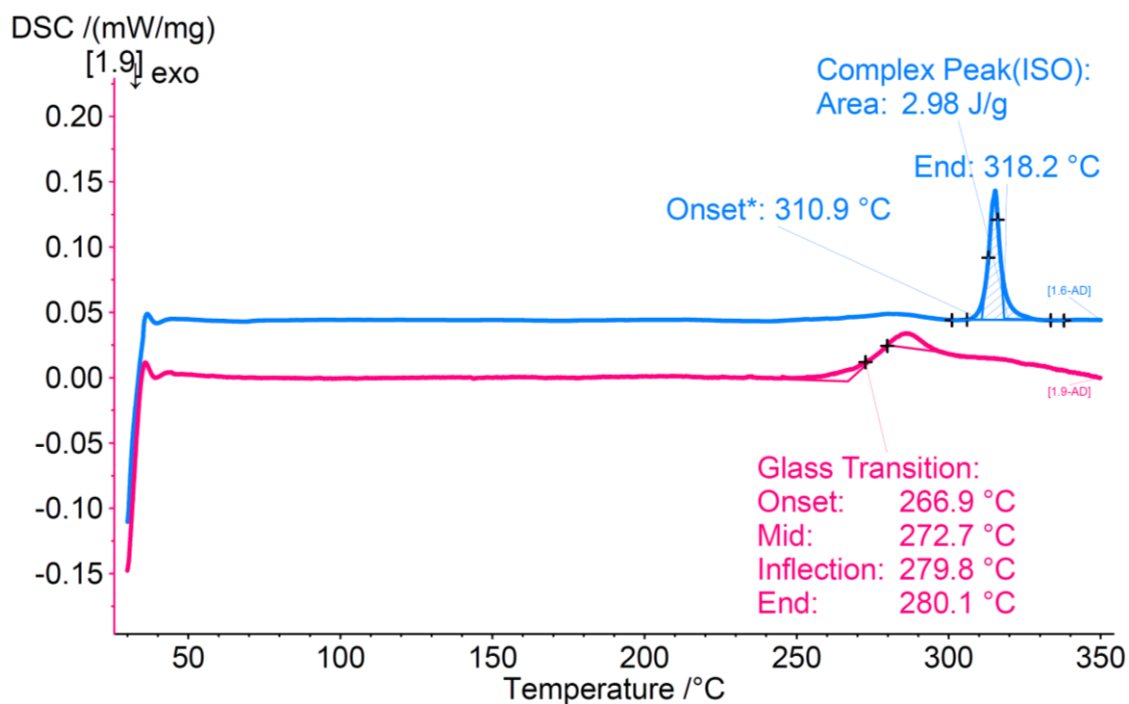


**Figure S12:** Analysis of DSC of crystalline ZIF-UC-7 with *in-situ* activation step. The 2<sup>nd</sup> upscan to 350 °C with  $T_m = 318$  °C (blue) and 3<sup>rd</sup> upscan to 350 °C with  $T_g = 273$  °C (pink) are shown.  $T_m$  is taken as the offset (end) of melting whilst  $T_g$  is taken as the mid-point of the event. Heat flow curves are offset on the y axis for clarity.

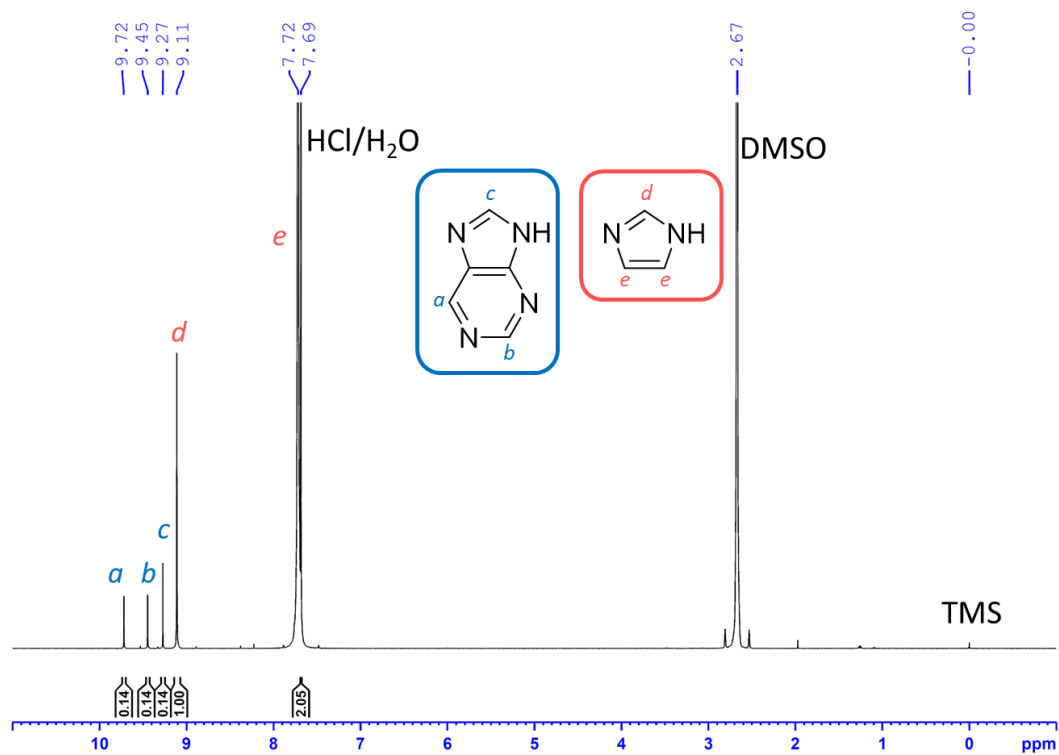


**Figure S13:**  $^1\text{H}$  NMR spectrum of ZIF-UC-7 post 350 °C.  $\delta\text{H}$  (500 MHz; DCI(35%)/D<sub>2</sub>O:DMSO-d<sub>6</sub> (1:5); Me<sub>4</sub>Si) 9.72 (1H, s, H<sub>a</sub>), 9.45 (1H, s, H<sub>b</sub>), 9.27 (1H, s, H<sub>c</sub>), 9.11 (1H, s, H<sub>d</sub>), 7.72 (2H, s, H<sub>e</sub>), 7.69 (H<sub>2</sub>O/HCl), 2.67 (DMSO), 0.00 (TMS).

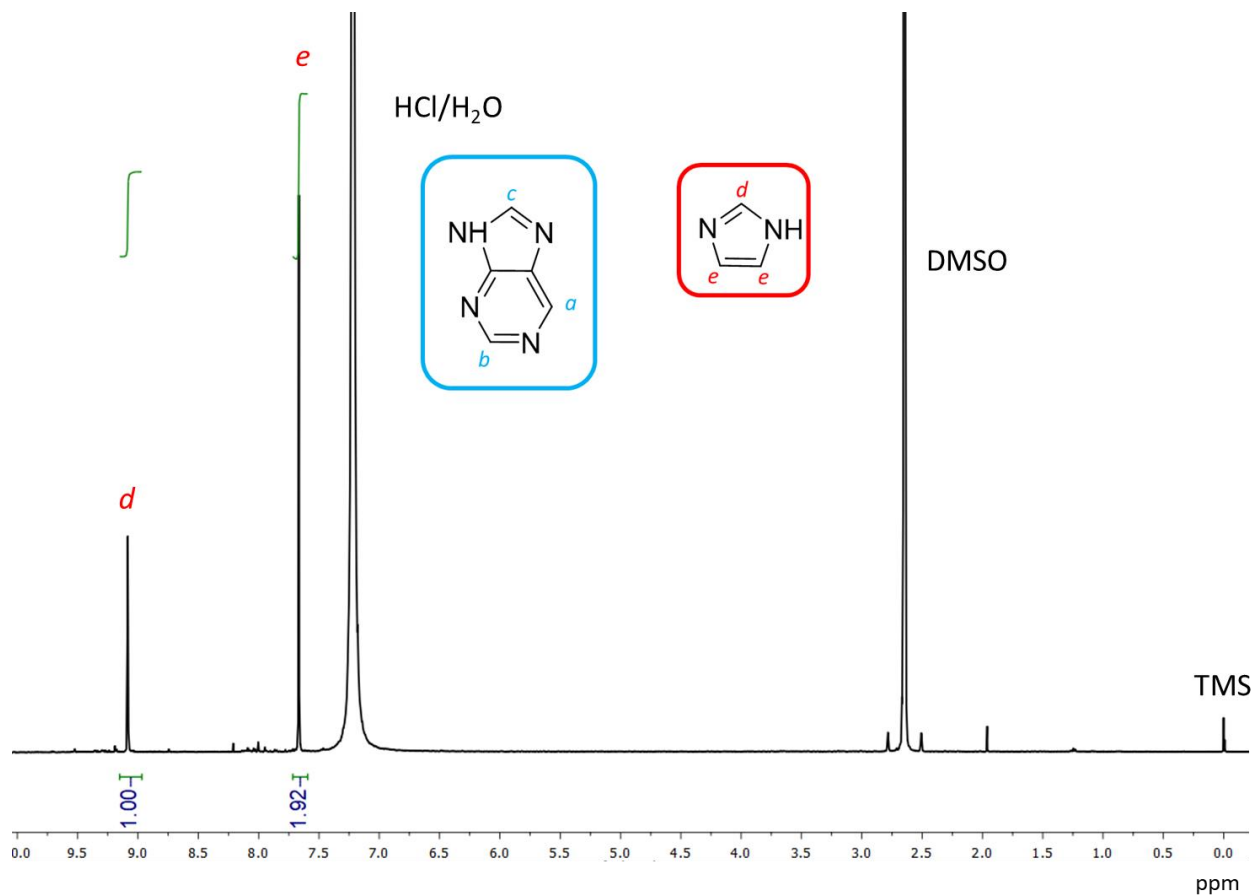


**Figure S14:**  $^1\text{H}$  NMR spectrum of ZIF-UC-7 post 550 °C.  $\delta\text{H}$  (500 MHz; DCI(35%)/D<sub>2</sub>O:DMSO-d<sub>6</sub> (1:5); Me<sub>4</sub>Si) 9.12 (1H, s, H<sub>d</sub>), 7.75 (2H, s, H<sub>e</sub>), 7.49 (H<sub>2</sub>O/HCl), 2.65 (DMSO), 0.00 (TMS). Signals of purine linker were not observed.

**Table S6:** CHN microanalysis of ZIF-UC-7 heated at 550 °C and comparison with the calculated formula

Sample	Mass (mg)	wt.% C	wt.% H	wt.% N
ZIF-UC-7	1.9134	34.41	2.69	26.82
ZIF-UC-7	1.8794	34.42	2.53	26.79
ZIF-UC-7	2.1285	34.43	2.54	26.84
Mean (ESD)	-	34.42 (0.01)	2.59 (0.08)	26.82 (0.02)
[Zn(pur) <sub>0.25</sub> (Im) <sub>1.75</sub> ]	-	36.43	3.65	29.41

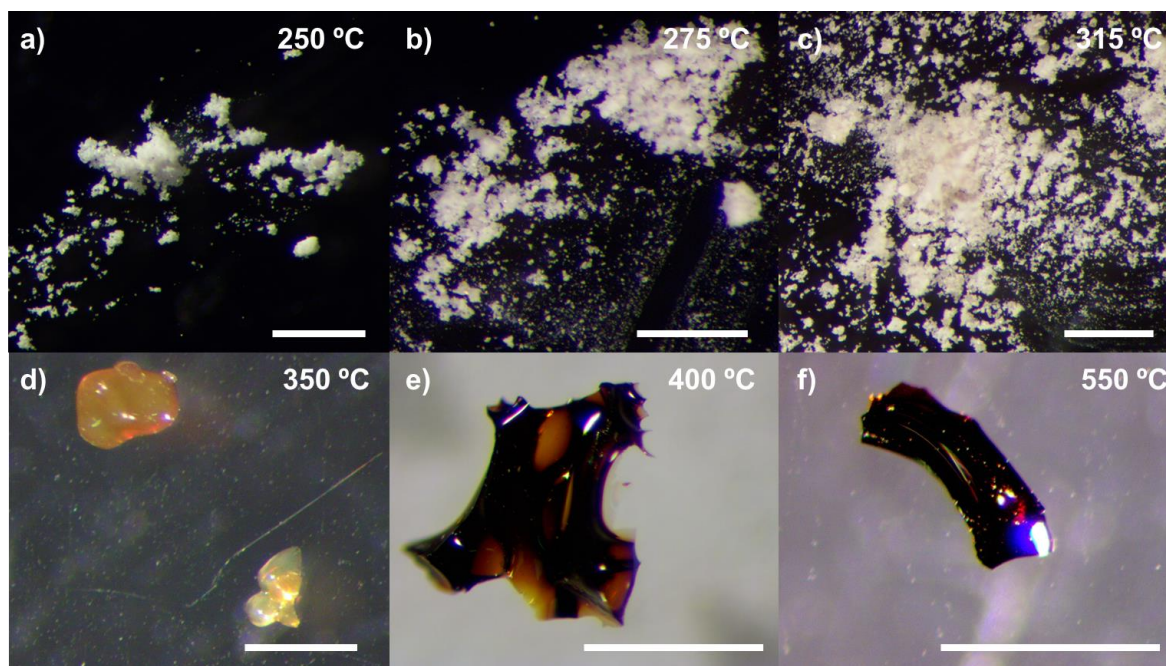


**Figure S15:** Optical images for ZIF-UC-7 polycrystalline after thermal treatment under argon atmosphere at 250, 275, 315, 350, 400 and 550 °C.

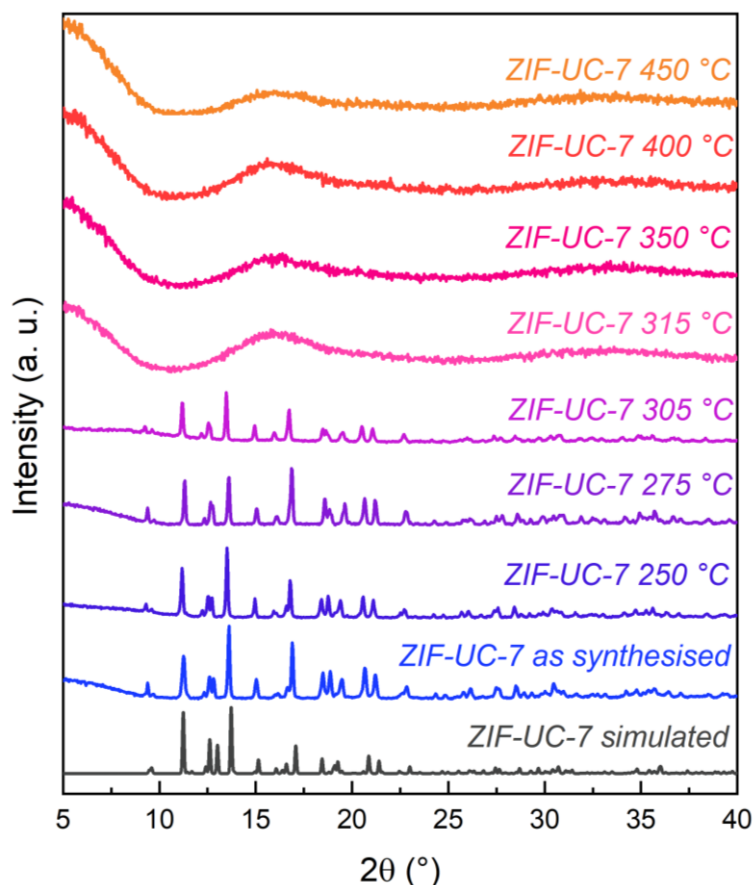


**Figure S16:** PXRD patterns between 5-40° of as prepared ZIF-UC-7 (blue) and ZIF-UC-7 heated to 250-450 °C (purple to orange) compared to the simulated diffraction pattern of ZIF-UC-7 (dark grey).

**Table S7:** Melting temperatures and thermodynamics of ZIF-UC-7 vs. reported values for other ZIFs

ZIF	$T_m$ (°C)	$T_g$ (°C)	$T_m$ (K)	$\Delta H_{fus}$ (J g <sup>-1</sup> )	$\Delta H_{fus}$ (kJ mol <sup>-1</sup> )	$\Delta S_{fus}$ (J K <sup>-1</sup> mol <sup>-1</sup> )
ZIF-UC-7	318	278	591	3.0	0.6	1.0
ZIF-UC-6 <sup>1</sup>	345	316	618	7.8	1.7	2.8
ZIF-UC-5 <sup>12</sup>	428	336	701	11.7	2.5	3.6
ZIF-UC-4 <sup>13</sup>	421	290	694	N/A	N/A	N/A
ZIF-UC-3 <sup>13</sup>	390	336	663	N/A	N/A	N/A
ZIF-UC-2 <sup>13</sup>	406	250	679	N/A	N/A	N/A
ZIF-62(Zn) <sup>14*</sup>	372-441	298-320	645-714	N/A	0.4-2.5	0.7-3.5
ZIF-62(Co) <sup>14**</sup>	398-420	260-290	659-705	N/A	0.8-2.6	1.3-3.7
TIF-4 <sup>12</sup>	440	350	713	15.3	3.2	4.5
[Co <sub>0.2</sub> Zn <sub>0.8</sub> (Im) <sub>1.95</sub> (blm) <sub>0.025</sub> (Clblm) <sub>0.025</sub> ] <sup>15</sup>	310	288	583	N/A	N/A	N/A

\* Compositions ZIF-62, [Zn(Im)<sub>2</sub>(blm)<sub>2-x</sub>], 0 ≤ x ≤ 0.35

\*\* Compositions ZIF-62, [Zn(Im)<sub>2</sub>(blm)<sub>2-x</sub>], 0.1 ≤ x ≤ 0.3

(Im = imidazolate, blm = benzylimidazolate, Clblm = 5-chlorobenzenimidazolate)

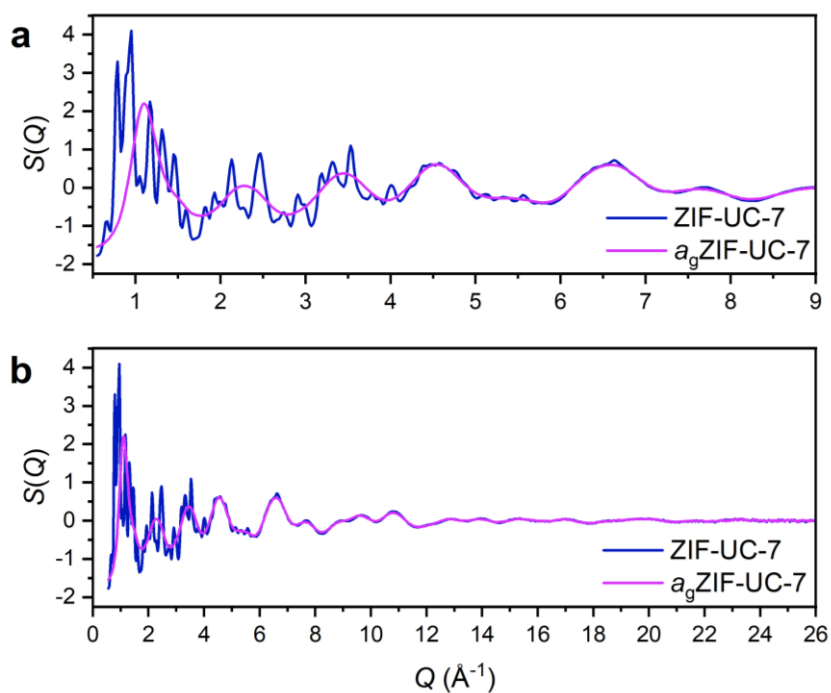


**Figure S17:** Total scattering structure factors of ZIF-UC-7 (blue) and  $a_g$ ZIF-UC-7 (purple). (a) Highlights differences in the low  $Q$  region between ZIF-UC-7 and  $a_g$ ZIF-UC-7 resulting from differences in their long-range order. (b) Shows the total scattering data collected for both materials in the full  $Q$  range up to a  $Q_{\text{max}} \approx 26 \text{ \AA}^{-1}$ . All processing of the total scattering data was performed using GudrunX following well documented procedures.<sup>8-10</sup>

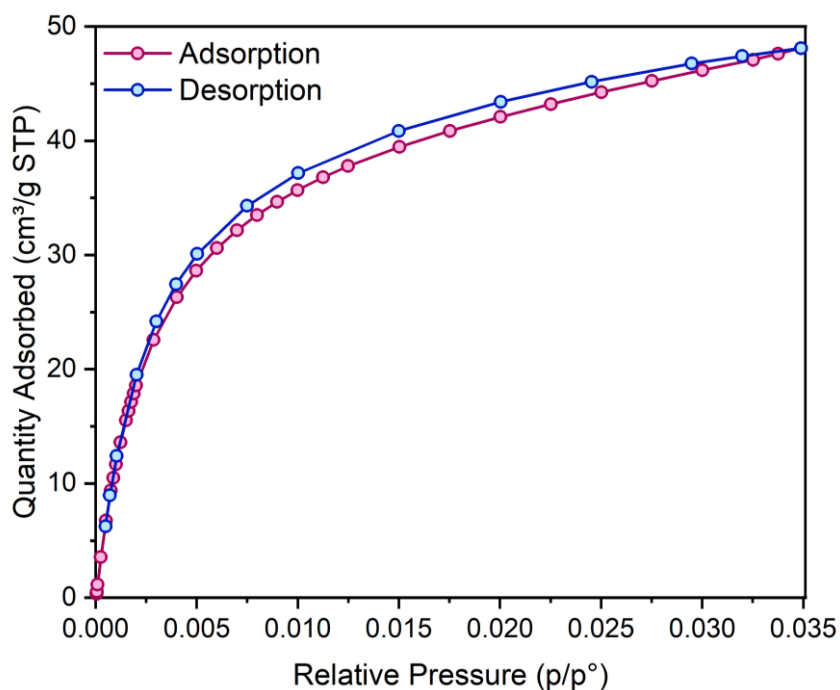


**Figure S18:** CO<sub>2</sub> adsorption (pink) and desorption (blue) isotherms collected on crystalline ZIF-UC-7 from 0-0.035  $p/p^0$ . Maximum gas uptake was determined using the Micromeritics MicroActive software package.

**Table S8:** CO<sub>2</sub> gas sorption results for crystalline ZIF-UC-7

Maximum CO <sub>2</sub> uptake (cm <sup>3</sup> g <sup>-1</sup> STP)	48.11
Maximum CO <sub>2</sub> uptake (mmol g <sup>-1</sup> )	2.15

**Table S9:** CO<sub>2</sub> gas sorption results for ZIF-UC-7 and  $a_g$ ZIF-UC-7 vs. reported values for other ZIFs with a similar structure and  $cag$  topology. All STP values were taken at a  $P/P^\circ$  value of 0.035.

ZIF crystalline	STP (cm <sup>3</sup> /g)	ZIF glass	STP (cm <sup>3</sup> /g)	Reference
ZIF-UC-7	48.11	ZIF-UC-7	18.94	This work
ZIF-UC-6	46.90	ZIF-UC-6	22.96	1
ZIF-UC-5	No data	ZIF-UC-5	No data	12
		$a_m[\text{Zn}(\text{Im})_{1.65}(\text{blm})_{0.35}]$	23.24	17
		$a_g[\text{Zn}(\text{Im})_{1.65}(\text{blm})_{0.35}]$	23.37	17
ZIF-62 (Co)	44.84	$a_g$ ZIF-62 (Co)	20.20	18

(Im = imidazolate, blm = benzylimidazolate)

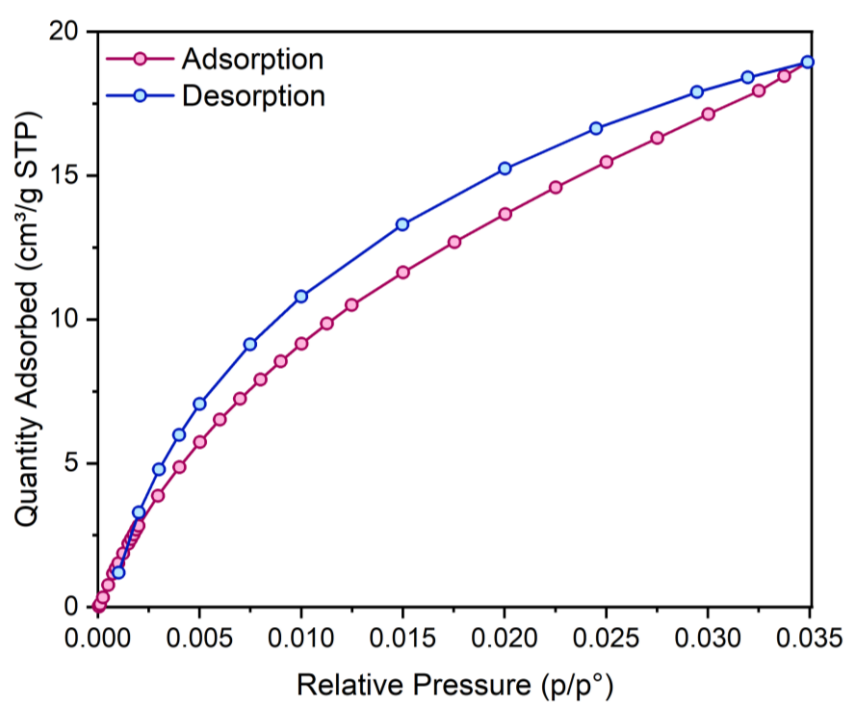


**Figure S19:** CO<sub>2</sub> adsorption (pink) and desorption (blue) isotherms collected on  $a_g$ ZIF-UC-7 from 0-0.035  $p/p^\circ$ .

**Table S10:** CO<sub>2</sub> gas sorption results for  $a_g$ ZIF-UC-7

Maximum CO <sub>2</sub> uptake (cm <sup>3</sup> g <sup>-1</sup> STP)	18.94
Maximum CO <sub>2</sub> uptake (mmol g <sup>-1</sup> )	0.85

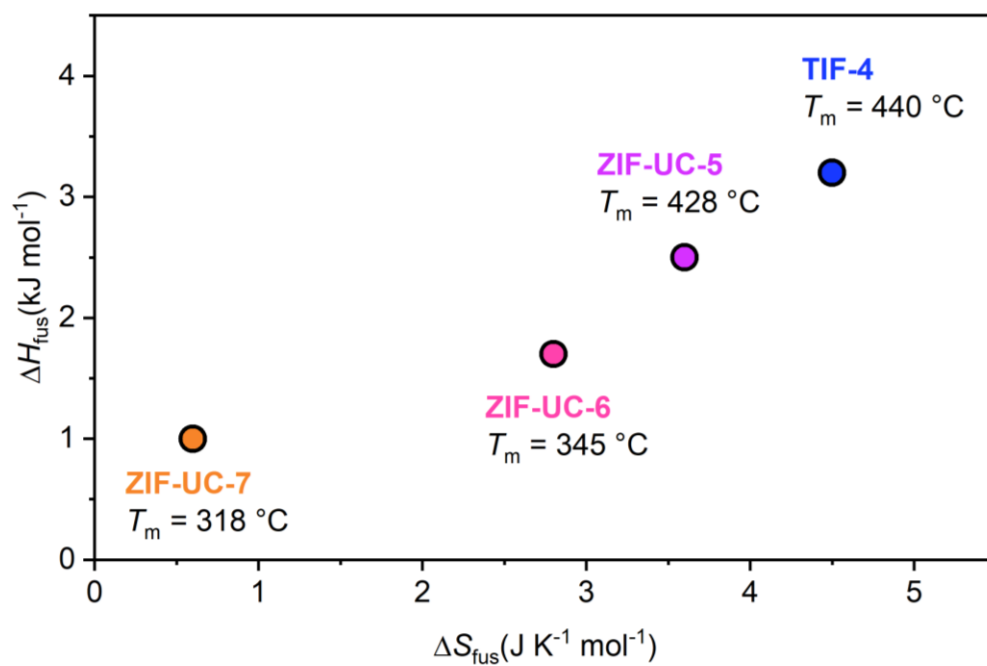


**Figure S20:** Enthalpy and entropy of fusion of ZIF-UC-7 compared to other ZIFs. Values were calculated based on the method reported by Mason *et al.*<sup>16</sup> The molar enthalpy was calculated using the molecular weight for the ZIF formula unit.

## References

- 1 A. M. Bumstead, I. Pakamorè, K. D. Richards, M. F. Thorne, S. S. Boyadjieva, C. Castillo-Blas, L. N. McHugh, A. F. Sapnik, D. S. Keeble, D. A. Keen, R. C. Evans, R. S. Forgan and T. D. Bennett, *Chem. Mater.*, 2022, **34**, 2187–2196.
- 2 G. M. Sheldrick, *Acta Crystallogr.*, 2015, **A71**, 3–8.
- 3 G. M. Sheldrick, *Acta Crystallogr.*, 2015, **C71**, 3–8.
- 4 O. V. Dolomanov, L. J. Bourhis, R. J. Gildea, J. A. K. Howard and H. Puschmann, *J. Appl. Crystallogr.*, 2009, **42**, 339–341.
- 5 A. L. Spek, *Acta Crystallogr. Sect. D Biol. Crystallogr.*, 2009, **65**, 148–155.
- 6 N. Kourkoumelis, in *ICDD Annual Spring Meetings*, ed. L. O'Neill, Cambridge University Press, Cambridge, 2013, pp. 137–148.
- 7 A. A. Coelho, *J. Appl. Crystallogr.*, 2018, **51**, 210–218.
- 8 A. K. Soper and E. R. Barney, *J. Appl. Crystallogr.*, 2011, **44**, 714–726.
- 9 A. K. Soper, *GudrunN and GudrunX: programs for correcting raw neutron and X-ray diffraction data to differential scattering cross section*, 2011.
- 10 D. A. Keen, *J. Appl. Crystallogr.*, 2001, **34**, 172–177.
- 11 C. A. Schneider, W. S. Rasband and K. W. Eliceiri, *Nat. Methods*, 2012, **9**, 671–675.
- 12 A. M. Bumstead, M. L. Rios Gomez, M. F. Thorne, A. F. Sapnik, L. Longley, J. M. Tuffnell, D. S. Keeble, D. A. Keen and T. D. Bennett, *CrystEngComm*, 2020, **22**, 3627–3637.
- 13 J. Hou, M. L. Ríos Gómez, A. Krajnc, A. McCaul, S. Li, A. M. Bumstead, A. F. Sapnik, Z. Deng, R. Lin, P. A. Chater, D. S. Keeble, D. A. Keen, D. Appadoo, B. Chan, V. Chen, G. Mali and T. D. Bennett, *J. Am. Chem. Soc.*, 2020, **142**, 3880–3890.
- 14 L. Frentzel-Beyme, M. Kloß, P. Kolodzeiski, R. Pallach and S. Henke, *J. Am. Chem. Soc.*, 2019, **141**, 12362–12371.
- 15 A. M. Bumstead, M. F. Thorne and T. D. Bennett, *Faraday Discuss.*, 2021, **225**, 210–225.
- 16 M. Liu, R. D. McGillicuddy, H. Vuong, S. Tao, A. H. Slavney, M. I. Gonzalez, S. J. L. Billinge and J. A. Mason, *J. Am. Chem. Soc.*, 2021, **143**, 2801–2811.
- 17 M. F. Thorne, C. Castillo-Blas, L. N. McHugh, A. M. Bumstead, G. Robertson, A. F. Sapnik, C. S. Coates, F. N. Sayed, C. P. Grey, D. A. Keen, M. Etter, I. da Silva, K. Užarević and T. D. Bennett, *Chem. Commun.*, , DOI:10.1039/D2CC04241J.
- 18 L. Frentzel-Beyme, M. Kloß, R. Pallach, S. Salamon, H. Moldenhauer, J. Landers, H. Wende, J. Debus and S. Henke, *J. Mater. Chem. A*, 2019, **7**, 985–990.